

Group-velocity-matching relationship in the process of third-harmonic generation

Yisheng Yang,^{1,2,*} Wei Han,¹ Wanguo Zheng,¹ Jichun Tan,² Fuquan Li,¹ Fang Wang,¹ Yong Xiang,¹ Keyu Li,¹ Bin Feng,¹ Huaiting Jia,¹ Dingxiang Cao,² and Jun Dong¹

¹Research Center of Laser Fusion, China Academy of Engineering Physics, P.O. Box 919-988, Mianyang 621900, China

²College of Science, National University of Defense Technology, Changsha 410073, China

(Received 16 July 2008; published 3 November 2008)

Based on the nonlinear coupling equations, the process of third-harmonic generation (THG) is investigated theoretically in temporal and frequency domains and a set of analytical expressions is derived under the plane-wave and pump undepletion approximations. The explicit formula characterizing the group-velocity-matching relationship in the process of THG is obtained. The group-velocity-matching relationship appears to be dependent on the pulse-duration ratio of fundamental (FH) to second-harmonic (SH) pulses. The THG mixing process in KDP crystals with input Gaussian pulses is numerically simulated, and the obtained results show that the conversion efficiency and conversion bandwidth can reach maximum when the formula is satisfied (i.e., zero group-velocity mismatch), and both will decrease rapidly when the formula is unsatisfied. Numerical results confirm the validity of our formula. Furthermore, with the increasing of the pulse-duration ratio of FH to SH pulses, the maximum bandwidth of generated TH pulses increases while maximum THG conversion efficiency decreases.

DOI: 10.1103/PhysRevA.78.053801

PACS number(s): 42.65.Ky, 42.65.Yj, 42.65.Lm

I. INTRODUCTION

Third-harmonic generation (THG) is a powerful technique to produce widely tunable and high-energy ultrashort laser pulses which have important applications in fields such as laser spectroscopy, inertial confinement fusion (ICF) [1,2], photolithography, and medical and biological uses. With the rapid development of ultrashort-pulse lasers in recent years, THG is attracting increasing interest. Unfortunately, due to the lack of adequate birefringence in nonlinear crystals, the THG conversion efficiency and conversion bandwidth are limited by the inevitable group-velocity mismatch (namely, temporal walk-off) in the process of THG, especially in the case of pulse duration of about 100 fs or shorter. Group-velocity mismatch causes the input pulses and the growing generated pulse to walk away from each other in a time domain while they propagate in nonlinear crystals. Thus, it leads to the generated pulse broadening, the spectral bandwidth narrowing, and the conversion efficiency decreasing.

In order to increase conversion efficiency and maintain the temporal shape of harmonic pulses as well as the spectrum in the THG process of ultrashort pulses, many specific approaches were proposed and demonstrated. For example, the so-called achromatic phase matching, which lets the waves with different frequency components propagate with their own phase-matching angles into the crystal by introducing angular dispersion, can satisfy the phase matching for the entire frequency component. THG with cascading crystals with opposite group-velocity walk-off can increase conversion efficiency to some extent [3–10]. Although the approaches mentioned above were demonstrated successfully to satisfy or compensate for the group-velocity mismatch in broadband second-harmonic generation (SHG) [11–19], they are not suitable in broadband THG because the group-velocity-matching (GVM) relationship is much more compli-

cated than that of SHG. As is well known, the perfect GVM relationship in the SHG process is “ $v_{g1}=v_{g2}$,” where v_{g1} and v_{g2} are the group velocities of fundamental and second-harmonic pulses, respectively. The GVM in this situation is also called the spectral noncritical phase matching [15,16]. Undoubtedly, the perfect GVM relationship in the THG process is “ $v_{g1}=v_{g2}=v_{g3}$,” where v_{g1} , v_{g2} , and v_{g3} are the group velocities of fundamental, second-harmonic, and third-harmonic pulses, respectively. However, according to the Sellmeier equations of various crystals [20], it is nearly impossible to satisfy the perfect GVM relationship. Here, we try to determine a proper GVM relationship of THG which can reflect the intrinsic properties of group velocities among three interacting waves.

In this paper, the temporal walk-off effect caused by group-velocity mismatch in the process of broadband THG is investigated in detail. Theoretical analyses of the nonlinear coupling equations in the temporal or the frequency domains are discussed in Sec. II. In Sec. III, the explicit formula characterizing the GVM relationship of THG is derived for Gaussian pulses. In Sec. IV, numerical simulation for verification is presented. Finally, Sec. V concludes the paper.

II. THEORETICAL SOLUTIONS TO THE NONLINEAR COUPLING EQUATIONS

The interacting waves in the THG process can be written in the form

$$E_n(z,t) = \frac{1}{2}A_n(z,t)\exp[i(k_n z - \omega_n t)] + \text{c.c.}, \quad (1)$$

where $E_1(z,t)$, $E_2(z,t)$, and $E_3(z,t)$ are the complex amplitudes of fundamental, second-harmonic, and third-harmonic pulses, respectively. Neglecting the effects of diffraction, spatial walk-off, and third-order nonlinearities, etc., the nonlinear coupled amplitude equations describing the third-harmonic generation under plane-wave approximation are [21]

*ysyang@nudt.edu.cn

$$\begin{aligned} \frac{\partial A_1(z,t)}{\partial z} + \beta_{11} \frac{\partial A_1(z,t)}{\partial t} + \frac{i}{2} \beta_{12} \frac{\partial^2 A_1(z,t)}{\partial t^2} + \alpha_1 A_1(z,t) \\ = \frac{i\omega_1 d_e}{n_1 c} A_3 A_2^* e^{i\Delta k_0 z}, \end{aligned} \quad (2a)$$

$$\begin{aligned} \frac{\partial A_2(z,t)}{\partial z} + \beta_{21} \frac{\partial A_2(z,t)}{\partial t} + \frac{i}{2} \beta_{22} \frac{\partial^2 A_2(z,t)}{\partial t^2} + \alpha_2 A_2(z,t) \\ = \frac{i\omega_2 d_e}{n_2 c} A_3 A_1^* e^{i\Delta k_0 z}, \end{aligned} \quad (2b)$$

$$\begin{aligned} \frac{\partial A_3(z,t)}{\partial z} + \beta_{31} \frac{\partial A_3(z,t)}{\partial t} + \frac{i}{2} \beta_{32} \frac{\partial^2 A_3(z,t)}{\partial t^2} + \alpha_3 A_3(z,t) \\ = \frac{i\omega_3 d_e}{n_3 c} A_1 A_2 e^{-i\Delta k_0 z}. \end{aligned} \quad (2c)$$

In the above equations, $\beta_{n1} = (\partial k_n / \partial \omega)_{\omega_n} \equiv v_{gn}^{-1}$ is the first-order group-velocity dispersion, and is equal to the inverse group velocity of the n th wave. $\beta_{n2} = (\partial^2 k_n / \partial \omega^2)_{\omega_n} \equiv \partial / \partial \omega (1 / v_{gn})$ is the second-order group-velocity dispersion (GVD), α_n is the linear loss term, and d_e is the nonlinear optical coefficient. $\Delta k_0 = k_{\omega_3} - k_{\omega_1} - k_{\omega_2}$ represents the original phase mismatch at the center frequencies, which is zero in the phase-matched case.

In order to solve the nonlinear coupled equations analytically, the pump undepletion is assumed (i.e., $|A_{3\omega}| \ll |A_{1\omega}|, |A_{2\omega}|$) which is satisfied usually due to the low THG conversion efficiency of ultrashort pulses. In this case, Eqs. (2) are simplified to be

$$\frac{\partial A_1(z,t)}{\partial z} + \beta_{11} \frac{\partial A_1(z,t)}{\partial t} + \frac{i}{2} \beta_{12} \frac{\partial^2 A_1(z,t)}{\partial t^2} + \alpha_1 A_1(z,t) = 0, \quad (3a)$$

$$\frac{\partial A_2(z,t)}{\partial z} + \beta_{21} \frac{\partial A_2(z,t)}{\partial t} + \frac{i}{2} \beta_{22} \frac{\partial^2 A_2(z,t)}{\partial t^2} + \alpha_2 A_2(z,t) = 0, \quad (3b)$$

$$\begin{aligned} \frac{\partial A_3(z,t)}{\partial z} + \beta_{31} \frac{\partial A_3(z,t)}{\partial t} + \frac{i}{2} \beta_{32} \frac{\partial^2 A_3(z,t)}{\partial t^2} + \alpha_3 A_3(z,t) \\ = \frac{i\omega_3 d_e}{n_3 c} A_1 A_2 e^{-i\Delta k_0 z}. \end{aligned} \quad (3c)$$

First, let us consider Eqs. (3a) and (3b). By transforming the coordinate (z, t) to the local coordinates $(z, T = t - z\beta_{11})$ and $(z, T' = t - z\beta_{21})$, and introducing normalized amplitudes $U_1(z, T)$, $U_2(z, T')$ through the definition $A_1(z, T) = \sqrt{I_1} e^{-\alpha_1 z} U_1(z, T)$, $A_2(z, T') = \sqrt{I_2} e^{-\alpha_2 z} U_2(z, T')$, where I_1 and I_2 are the intensities of the input fundamental (FH) and second-harmonic (SH) pulses, respectively, Eqs. (3a) and (3b) are simplified to

$$\frac{\partial U_1(z, T)}{\partial z} + \frac{i}{2} \beta_{12} \frac{\partial^2 U_1(z, T)}{\partial T^2} = 0, \quad (4a)$$

$$\frac{\partial U_2(z, T')}{\partial z} + \frac{i}{2} \beta_{22} \frac{\partial^2 U_2(z, T')}{\partial T'^2} = 0. \quad (4b)$$

Substituting the Fourier transformations of $U_1(z, T)$ and $U_2(z, T')$ into Eqs. (4), they can be easily solved. The amplitude expressions of FH and SH pulses in the temporal domain are as follows:

$$\begin{aligned} A_1(z, T) &= \sqrt{I_1} e^{-\alpha_1 z} U_1(z, T) \\ &= \sqrt{I_1} e^{-\alpha_1 z} \frac{1}{2\pi} \int_{-\infty}^{\infty} \left(\int_{-\infty}^{\infty} U_1(0, T) \exp(i\omega T) dT \right) \\ &\quad \times \exp\left(\frac{i}{2} \beta_{12} \omega^2 z - i\omega T\right) d\omega, \end{aligned} \quad (5a)$$

$$\begin{aligned} A_2(z, T') &= \sqrt{I_2} e^{-\alpha_2 z} \frac{1}{2\pi} \int_{-\infty}^{\infty} \left(\int_{-\infty}^{\infty} U_2(0, T') \exp(i\omega T') dT' \right) \\ &\quad \times \exp\left(\frac{i}{2} \beta_{22} \omega^2 z - i\omega T'\right) d\omega. \end{aligned} \quad (5b)$$

Similarly, the local coordinate $(z, \tau = t - z\beta_{31})$ and the amplitude $W_3(z, \tau)$ defined by $A_3(z, \tau) = e^{-\alpha_3 z} W_3(z, \tau)$ are introduced into Eq. (3c) which includes the nonlinear interaction term on the right-hand side. Then Eq. (3c) is simplified to

$$\begin{aligned} \frac{\partial W_3(z, \tau)}{\partial z} + \frac{i}{2} \beta_{32} \frac{\partial^2 W_3(z, \tau)}{\partial \tau^2} \\ = \frac{i\omega_3 d_e}{n_3 c} A_1(z, \tau) A_2(z, \tau) \exp(-i\Delta k_0 + \alpha_3 z), \end{aligned} \quad (6)$$

where $A_1(z, \tau)$ and $A_2(z, \tau)$ can be obtained by substituting $T = \tau + z\beta_{11}$ and $T' = \tau + z\beta_{21}$ into Eqs. (5a) and (5b), respectively. The $v_1 = \beta_{31} - \beta_{11}$, $v_2 = \beta_{31} - \beta_{21}$ are the so-called group-velocity mismatches.

Substituting the Fourier transformation of $W_3(z, \tau)$ [i.e., $\tilde{W}_3(z, \omega) = \mathbf{F}\{W_3(z, \tau)\}$] into Eq. (6), it becomes a nonhomogeneous differential equation in the frequency domain,

$$\frac{\partial \tilde{W}_3(z, \omega)}{\partial z} = \frac{i}{2} \beta_{32} \omega^2 \tilde{W}_3(z, \omega) + \tilde{f}(z, \omega), \quad (7)$$

where

$$\tilde{f}(z, \omega) = \frac{i\omega_3 d_e}{n_3 c} e^{(-i\Delta k_0 z + \alpha_3 z)} \int_{-\infty}^{\infty} [A_1(z, \tau) A_2(z, \tau)] e^{i\omega \tau} d\tau. \quad (8)$$

Through the general solution to the nonhomogeneous differential equations, we can easily obtain the solution of Eq. (7),

$$\begin{aligned} \tilde{W}_3(z, \omega) &= \frac{i\omega_3 d_e}{n_3 c} e^{(i/2)\beta_{32}\omega^2 z} \int_0^z \int_{-\infty}^{\infty} [A_1(\xi, \tau) A_2(\xi, \tau)] e^{i\omega \tau} d\tau \\ &\quad \times e^{[-i\Delta k_0 + \alpha_3 - (i/2)\beta_{32}\omega^2]\xi} d\xi. \end{aligned} \quad (9)$$

Thus, the amplitude expression of TH pulses in the frequency domain is

$$\begin{aligned} \tilde{A}_3(z, \omega) &= \frac{i\omega_3 d_e}{n_3 c} e^{[(i/2)\beta_{32}\omega^2 - \alpha_3]z} \int_0^z \int_{-\infty}^{\infty} [A_1(\xi, \tau) A_2(\xi, \tau)] e^{i\omega\tau} d\tau \\ &\quad \times e^{[-i\Delta k_0 + \alpha_3 - (i/2)\beta_{32}\omega^2]z} d\xi. \end{aligned} \quad (10)$$

Equations (5) and (10) are the general amplitude solutions to the three-wave nonlinear coupling equations.

III. GROUP-VELOCITY-MATCHING RELATIONSHIP IN THE CASE OF GAUSSIAN PULSES

Just from Eqs. (5) and (10) we cannot find any relationship among group velocities of interacting waves; we need to integrate Eqs. (5) and (10) to more explicit analytical expressions for some specific cases. In this section, we consider a simple case of Gaussian pulses for which the normalized incident FH and SH fields are given by

$$U_1(0, t) = \exp\left(-\frac{1+iC_1}{2} \frac{t^2}{T_1^2}\right), \quad (11a)$$

$$U_2(0, t) = \exp\left(-\frac{1+iC_2}{2} \frac{t^2}{T_2^2}\right), \quad (11b)$$

where $T_{1,2}$ are the half-widths at the $1/e$ intensity, and $C_{1,2}$ are the chirp parameters. (The subscripts 1 and 2 refer to FH and SH pulses, respectively).

Substituting Eqs. (11) into Eq. (5), we obtain the propagating FH and SH fields in the temporal domain at the length of z in crystals, as follows:

$$A_1(z, T) = \sqrt{I_1} e^{-\alpha_1 z} \frac{T_1}{H_1} \exp(-aT^2), \quad (12a)$$

$$A_2(z, T') = \sqrt{I_2} e^{-\alpha_2 z} \frac{T_2}{H_2} \exp(-bT'^2), \quad (12b)$$

where, for simplicity, $H_1^2 = T_1^2 - i\beta_{12}z(1+iC_1)$, $H_2^2 = T_2^2 - i\beta_{22}z(1+iC_2)$, and $a = \frac{1+iC_1}{2H_1^2}$, $b = \frac{1+iC_2}{2H_2^2}$. Using the substitutions $T = \tau + zv_1$ and $T' = \tau + zv_2$, the generated TH fields in the frequency domain accordingly take the form

$$\tilde{A}_3(z, \omega) = \sqrt{I_1 I_2} \frac{i\omega_3 d_e}{n_3 c} e^{[(i/2)\beta_{32}\omega^2 - \alpha_3]z} \int_0^z \int_{-\infty}^{\infty} \exp[-a(\tau + \xi v_1)^2 - b(\tau + \xi v_2)^2] e^{i\omega\tau} d\tau \frac{T_1 T_2}{H_1 H_2} e^{[-i\Delta k_0 + \alpha_3 - \alpha_1 - \alpha_2 - (i/2)\beta_{32}\omega^2]z} d\xi. \quad (13)$$

The second integral of Eq. (13) can be deduced as follows:

$$\begin{aligned} \int_{-\infty}^{\infty} \exp[-a(\tau + \xi v_1)^2 - b(\tau + \xi v_2)^2] e^{i\omega\tau} d\tau &= \int_{-\infty}^{\infty} \exp\left\{-a(1+x) \left[\left(\tau + \frac{\xi}{1+x}(v_1 + xv_2)\right)^2 + \frac{x\xi^2}{(1+x)^2}(v_1 - v_2)^2\right]\right\} e^{i\omega\tau} d\tau \\ &= \sqrt{\frac{\pi}{a(1+x)}} \exp\left(-\frac{\omega^2}{4a(1+x)}\right) \exp\left(-i\omega \frac{\xi}{1+x}(v_1 + xv_2)\right) \exp\left(-a \frac{x\xi^2}{1+x}(v_1 - v_2)^2\right), \end{aligned} \quad (14)$$

where $x = \frac{b}{a} = \frac{H_1^2(1+iC_2)}{H_2^2(1+iC_1)}$ is a parameter about pulse durations and chirp parameters of FH and SH pulses. Substituting Eq. (14) into Eq. (13) and neglecting absorption, the generated TH fields in the frequency domain $\tilde{A}_3(z, \omega)$ becomes

$$\tilde{A}_3(z, \omega) = \sqrt{I_1 I_2} \frac{i\omega_3 d_e}{n_3 c} \frac{T_1 T_2}{H_1 H_2} \sqrt{\frac{\pi}{a(1+x)}} \exp\left(-\frac{\omega^2}{4a(1+x)}\right) e^{(i/2)\beta_{32}\omega^2 z} \int_0^z \exp\left(-a \frac{1}{1+1/x}(v_1 - v_2)^2 \xi^2\right) \exp[-i\Delta k(\omega)\xi] d\xi, \quad (15)$$

where $\Delta k(\omega)$ is the total phase mismatch of the THG process, which can be written as

$$\Delta k(\omega) = \Delta k_0 + \frac{1}{1+x}(v_1 + xv_2)\omega + \frac{1}{2}\beta_{32}\omega^2. \quad (16)$$

If group velocities of FH and SH pulses are the same (accordingly $v_1 = v_2$), $\tilde{A}_3(z, \omega)$ is

$$\tilde{A}_3(z, \omega) = \sqrt{I_1 I_2} \frac{i\omega_3 d_e}{n_3 c} \frac{T_1 T_2}{H_1 H_2} \sqrt{\frac{\pi}{a(1+x)}} \exp\left(-\frac{\omega^2}{4a(1+x)}\right) e^{(i/2)\beta_{32}\omega^2 z} \frac{i}{\Delta k(\omega)} \{\exp[-i\Delta k(\omega)z] - 1\}. \quad (17)$$

If group velocities of FH and SH pulses are not the same, by substituting $m = a \frac{1}{1+1/x}(v_1 - v_2)^2$ into Eq. (15), $\tilde{A}_3(z, \omega)$ becomes

$$\tilde{A}_3(z, \omega) = \frac{1}{4} \sqrt{I_1 I_2} \frac{i\omega_3 d_e}{n_3 c} \frac{T_1 T_2}{H_1 H_2} \sqrt{\frac{\pi}{a(1+x)}} \exp\left(-\frac{\omega^2}{4a(1+x)}\right) e^{(i/2)\beta_{32}\omega^2 z} \sqrt{\frac{\pi}{m}} \exp\left((\sigma - 1) \frac{\Delta k^2(\omega)}{4m}\right) (1 - \exp\{-\sigma[mz^2 + i\Delta k(\omega)z]\}), \quad (18)$$

where the value of σ is $1 < \sigma < 2$ [see the solution of the integration $\int_0^z \exp(-ax^2)dx$].

Equation (16) indicates that the total phase mismatch includes the original phase mismatch between center frequencies and phase mismatches induced by group-velocity mismatches $v_{1,2}$ and second-order GVD β_{32} . Attention must be drawn to the second term of Eq. (16). It appears that if the group-velocity mismatches $v_{1,2}$ satisfy the equality $v_1 + xv_2 = 0$, then the total phase mismatch becomes $\frac{1}{2}\beta_{32}\omega^2$ and is only affected by the second-order GVD of a generated TH pulse for the phase-matched case ($\Delta k_0 = 0$). Using the definition of $v_{1,2}$ in Sec. II, the equality $v_1 + xv_2 = 0$ becomes

$$\frac{1+x}{v_{g3}} = \frac{1}{v_{g1}} + \frac{x}{v_{g2}}, \quad (19)$$

which is the explicit formula characterizing the GVM relationship of THG in the case of Gaussian pulses.

According to Eq. (19), we can find that the GVM relationship of interacting waves in the THG process is strongly dependent on the parameter x . For transform-limited pulses, i.e., $C_{1,2} = 0$, if the second-order GVD of FH and SH pulses β_{12} and β_{22} are negligible, the parameter x is approximately equal to $\frac{T_1^2}{T_2^2}$, which is the square of the pulse duration ratio of FH to SH pulses.

What is more interesting, the explicit GVM relationship derived in the THG process is also suitable for the SHG process. As in the SHG process (type-I SHG), v_{g1} , v_{g2} both represent the group velocity of the FH pulse, v_{g3} represents the group velocity of the SH pulse, and the ratio x is equal to 1, hence the GVM relationship in the SHG process becomes $\frac{2}{v_{g3}} = \frac{1}{v_{g1}} + \frac{1}{v_{g2}}$, i.e., $v_{SH} = v_{FH}$, which is the same as the results mentioned in Refs. [15,16].

In the next section, numerical simulation will be done to verify the validity of the GVM relationship of THG and will be compared with the above analytical results.

IV. NUMERICAL SIMULATION AND DISCUSSION

In order to check the validity of the GVM relationship of THG [i.e., Eq. (19)], the mixing process of THG in type-II KDP crystals is simulated based on the split-step Fourier-transform approach and the fourth-order Runge-Kutta integral method. The input FH and SH fields adopt the following Gaussian temporal profiles:

$$A_1(t) = I_1 \exp\left(-\frac{1+iC_1}{2} \frac{t^2}{T_1^2}\right), \quad (20a)$$

$$A_2(t) = I_2 \exp\left(-\frac{1+iC_2}{2} \frac{t^2}{T_2^2}\right), \quad (20b)$$

where chirp parameters $C_{1,2}$ are both set to be zero and peak intensities of FH and SH fields $I_{1,2}$ are 1 GW/cm^2 and $I_2 = 2 \text{ GW/cm}^2$, respectively. Under the pump undepletion approximation, crystal length L_D is limited to be smaller than the dispersion length of the TH pulse; here L_D is selected to be 2 mm. The time scale is set to be from $-64T_1$ to $64T_1$ in simulation. For simplicity, absorption and the second-

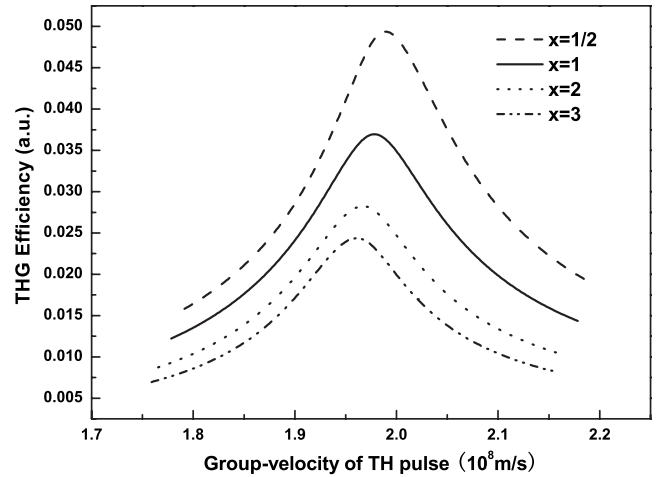


FIG. 1. THG conversion efficiency along with group velocity of TH pulse in the case of different pulse-duration ratio x .

higher-order GVD are assumed to be negligible.

We first investigate the dependence of THG conversion efficiency on the group velocity of a generated TH pulse for various pulse duration ratio x (i.e., $\frac{T_1^2}{T_2^2}$). In the numerical simulations, the pulse duration of the FH pulse T_1 is fixed to be 200 fs, thus different pulse duration T_2 of the SH pulse can result in a different value of ratio x . At the center fundamental wavelength $\lambda_{1\omega} = 1053 \text{ nm}$, the group velocities of input FH and SH pulses v_{g1} and v_{g2} are $2.01795 \times 10^8 \text{ m/s}$ and $1.94015 \times 10^8 \text{ m/s}$, respectively. Thus, at a fixed value of ratio x , only a particular value of v_{g3} can satisfy Eq. (19), in which case the highest THG conversion efficiency and broadest TH bandwidth can be obtained.

Figure 1 presents the curves of THG conversion efficiency versus the group velocities of a generated TH pulse in the case of a different ratio x . The THG conversion efficiency is defined as $\eta = \frac{E_{3\omega}}{E_{1\omega} + E_{2\omega}}$ and each point in the curve is the highest THG efficiency that can be obtained in a fixed status (i.e., fixed v_{g1} , v_{g2} , and v_{g3}). Four curves in Fig. 1 are corre-

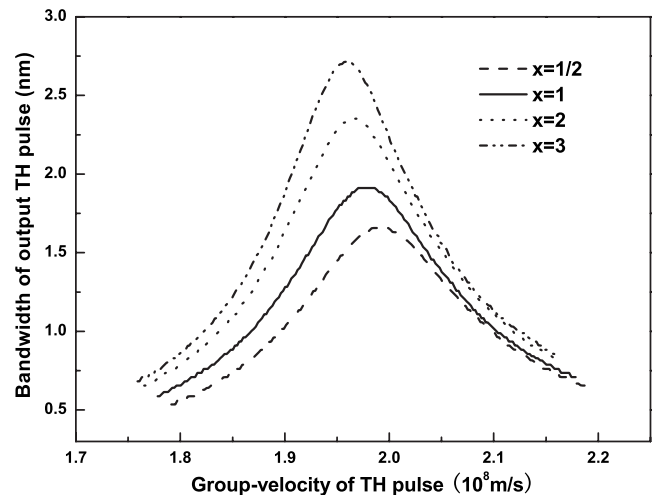


FIG. 2. Bandwidth of generated TH pulses along with group velocity of TH pulse in the case of different pulse-duration ratio x .

TABLE I. Comparison of theoretical and numerical data in the case of different pulse-duration ratio x .

Pulse-duration ratio $x = T_1^2 : T_2^2$	Formula $\frac{1+x}{v_{g3}} = \frac{1}{v_{g1}} + \frac{x}{v_{g2}}$	Theoretical value of v_{g3} (10^8 m/s)	Numerical value of v_{g3} (10^8 m/s)	Maximum THG efficiency (%)	Maximum bandwidth (nm)
1/2	$\frac{3}{v_{g3}} = \frac{2}{v_{g1}} + \frac{1}{v_{g2}}$	1.9913	1.9893	4.9	1.66
1	$\frac{2}{v_{g3}} = \frac{1}{v_{g1}} + \frac{1}{v_{g2}}$	1.9783	1.9783	3.7	1.91
2	$\frac{3}{v_{g3}} = \frac{1}{v_{g1}} + \frac{2}{v_{g2}}$	1.9654	1.9674	2.8	2.36
3	$\frac{4}{v_{g3}} = \frac{1}{v_{g1}} + \frac{3}{v_{g2}}$	1.9590	1.9610	2.4	2.72

sponding to the value of ratio x to be 1/2, 1, 2, and 3, respectively. In Fig. 2, curves of bandwidth of output TH pulses corresponding with conversion efficiency in Fig. 1 along with the group velocities of TH pulses are shown.

As shown in Figs. 1 and 2, the THG conversion efficiency and bandwidth of TH pulses both can reach maximum at a particular group velocity of the generated TH pulse, and both fall down rapidly when it is away from that particular group velocity. What is more important, with the increasing of pulse-duration ratio x , the maximum bandwidth of generated TH pulses will increase while the maximum THG conversion efficiency will decrease exponentially. This result is consistent with the qualitative conclusion made in Sec. III. Thus, in practical cases, different demands for high conversion efficiency or broad conversion bandwidth can be realized by selecting a proper value of parameter x .

Furthermore, in order to confirm the explicit formula expressed by Eq. (19), the theoretical data of group velocity of TH pulses calculated by (19) and numerical data accessed from Figs. 1 and 2 are listed and compared in Table I.

From Table I, we can find that the theoretical values of the group velocity of TH pulses are very close to the numerical ones, which confirms the validity of our formula describing group-velocity matching of three-coupling waves. Let us focus on Eq. (19); it is interesting that if the group velocities of input FH and SH pulses are the same, then $v_{g1} = v_{g2} = v_{g3}$, which corresponds to the case of perfect group-velocity matched. Otherwise, if $v_{g1} > v_{g2}$, then

$$\begin{aligned} \frac{1+x}{v_{g1}} &= \frac{1}{v_{g1}} + \frac{x}{v_{g1}} < \frac{1+x}{v_{g3}} = \frac{1}{v_{g1}} + \frac{x}{v_{g2}} < \frac{1}{v_{g2}} + \frac{x}{v_{g2}} \\ &= \frac{1+x}{v_{g2}} \quad (\text{i.e., } v_{g1} > v_{g3} > v_{g2}) \end{aligned} \quad (21)$$

or if $v_{g1} < v_{g2}$, then

$$v_{g1} < v_{g3} < v_{g2}. \quad (22)$$

Both results indicate that the generated TH pulse should be located between the FH and SH pulses through the whole propagation in crystals so that the energy of different waves can be coupled sufficiently and the group-velocity matching of THG can be realized.

V. CONCLUSION

The temporal walk-off effect caused by group-velocity mismatch in the process of broadband third-harmonic generation is investigated analytically and numerically. A set of analytical expressions of interacting waves for the general case is derived under the plane-wave and pump undepletion approximations, and an explicit formula characterizing the group-velocity-matching relationship in the process of THG is obtained for Gaussian pulses. The THG mixing process with Gaussian pulses input is numerically simulated in type-II KDP crystals. Comparison between theoretical group velocities of TH pulses calculated by our formula and numerical ones appears that THG conversion efficiency and bandwidth both can reach maximum when the formula is satisfied and both fall down rapidly when it is not satisfied, which confirms the validity of our formula. Meanwhile, with the increasing of pulse-duration ratio x , the maximum bandwidths of generated TH pulses increase while the maximum THG conversion efficiencies decrease.

This formula is useful for compensating for the group-velocity mismatch in the process of ultrashort third-harmonic generation such as finding nonlinear crystals with proper dispersive parameters and choosing effective group-velocity-matching methods, etc.

ACKNOWLEDGMENTS

This work was partially supported by the National Natural Science Foundation of China (Grant No. 60708007), and the Science and Technology Foundation of Chinese State Key Laboratory of High Temperature and Density Plasma Physics (Grant No. 9140C6803010802).

- [1] M. A. Henebian, P. J. Wegner, D. R. Speck, C. Bibeau, R. B. Ehrlich, C. W. Laumann, J. K. Lawson, and T. L. Weiland, *Proc. SPIE* **1415**, 90 (1991).
- [2] A. Babushkin, R. Craxton, S. Oskoui, M. Guardalben, R. L. Keck, and W. Seka, *Proc. SPIE* **3492**, 406 (1999).
- [3] A. P. Baronavski, H. D. Ladouceur, and J. K. Shaw, *IEEE J. Quantum Electron.* **29**, 580 (1993).
- [4] T. Zhang, Y. Kato, and H. Daido, *IEEE J. Quantum Electron.* **32**, 127 (1996).
- [5] D. Eimerl, J. M. Auerbach, C. E. Barker, D. Milam, and P. W. Milonni, *Opt. Lett.* **22**, 1208 (1997).
- [6] K. Osvay and I. N. Ross, *Opt. Commun.* **166**, 113 (1999).
- [7] F. Raoult, A. C. L. Boscheron, D. Husson, C. Rouyer, and C. Sauteret, *Opt. Lett.* **24**, 354 (1999).
- [8] Y. Qin, S. Tang, H. Su, and H. Guo, *Phys. Rev. A* **70**, 045803 (2004).
- [9] G. Feng, H. Zhao, J. Chen, P. Ying, J. Han, Q. Zhu, and X. Zhang, *Proc. SPIE* **5867**, 58670A (2005).
- [10] H. Liu, W. Zhao, Y. Yang, H. Wang, Y. Wang, and G. Chen, *Appl. Phys. B: Lasers Opt.* **82**, 585 (2006).
- [11] K. Hayata and M. Koshiba, *Appl. Phys. Lett.* **62**, 2188 (1993).
- [12] E. Sidick, A. Knoesen, and A. Dienes, *Opt. Lett.* **19**, 266 (1994).
- [13] H. Wang and A. Weiner, *IEEE J. Quantum Electron.* **39**, 1600 (2003).
- [14] N. E. Yu, S. Kurimura, K. Kitamura, J. H. Ro, M. Cha, S. Ashihara, T. Shimura, K. Kuroda, and T. Taira, *Appl. Phys. Lett.* **82**, 3388 (2003).
- [15] H. Zhu, T. Wang, W. Zheng, P. Yuan, L. Qian, and D. Fan, *Opt. Express* **12**, 2150 (2004).
- [16] X. Xiao, C. Yang, S. Gao, and H. Miao, *IEEE J. Quantum Electron.* **41**, 85 (2005).
- [17] A. M. Schober, M. Charbonneau-Lefort, and M. M. Fejer, *J. Opt. Soc. Am. B* **22**, 1699 (2005).
- [18] J. Luo, Y. Wang, W. Liang, J. Fonseca-Campos, and C. Xu, *Proc. SPIE* **6343**, 634349 (2006).
- [19] B. Morten, L. Jesper, B. Ole, and B. Anders, *8th International Conference on Transparent Optical Networks* (IEEE, Piscataway, NJ, 2006), pp. 49–54.
- [20] K. W. Kirby and L. G. Deshazer, *J. Opt. Soc. Am. B* **4**, 1072 (1987).
- [21] J. A. Armstrong, N. Bloembergen, J. Ducuing, and P. S. Pershan, *Phys. Rev.* **127**, 1918 (1962).